

Supplementary Information for

JAK-STAT Pathway Activation in Malignant and Non-Malignant Cells Contributes to MPN Pathogenesis and Therapeutic Response

Maria Kleppe^{1*}, Minsuk Kwak^{2*}, Priya Koppikar¹, Markus Riester³, Matthew Keller¹, Lennart Bastian¹, Todd Hricik¹, Neha Bhagwat^{1,4}, Anna Sophia McKenney^{1,4,5}, Efthymia Papalexli¹, Omar Abdel-Wahab^{1,6}, Raajit Rampal^{1,6}, Sachie Marubayashi¹, Jonathan J. Chen², Vincent Romanet⁷, Jordan S. Fridman⁸, Jacqueline Bromberg⁹, Julie Teruya-Feldstein¹⁰, Masato Murakami⁷, Thomas Radimerski⁷, Franziska Michor³, Rong Fan^{2,9,11,12}, and Ross L. Levine^{1,4,6,12}.

¹Human Oncology and Pathogenesis Program, Memorial Sloan-Kettering Cancer Center, New York, New York, USA

²Department of Biomedical Engineering, Yale University, New Haven, Connecticut, USA

³Department of Biostatistics and Computational Biology, Dana-Farber Cancer Institute, and Department of Biostatistics, Harvard School of Public Health, Boston, Massachusetts, USA

⁴Gerstner Sloan-Kettering Graduate School of Biomedical Sciences, New York, New York, USA

⁵Weill Cornell/Rockefeller/Sloan-Kettering Tri-Institutional MD-PhD Program, New York, New York, USA

⁶Leukemia Service, Department of Medicine, Memorial Sloan-Kettering Cancer Center, New York, New York, USA

⁷Disease Area Oncology, Novartis Institutes for BioMedical Research, Basel, Switzerland

⁸Incyte Corporation, Wilmington, Delaware, US

⁹Breast Cancer Service, Department of Medicine, Memorial Sloan-Kettering Cancer Center, New York, New York, USA

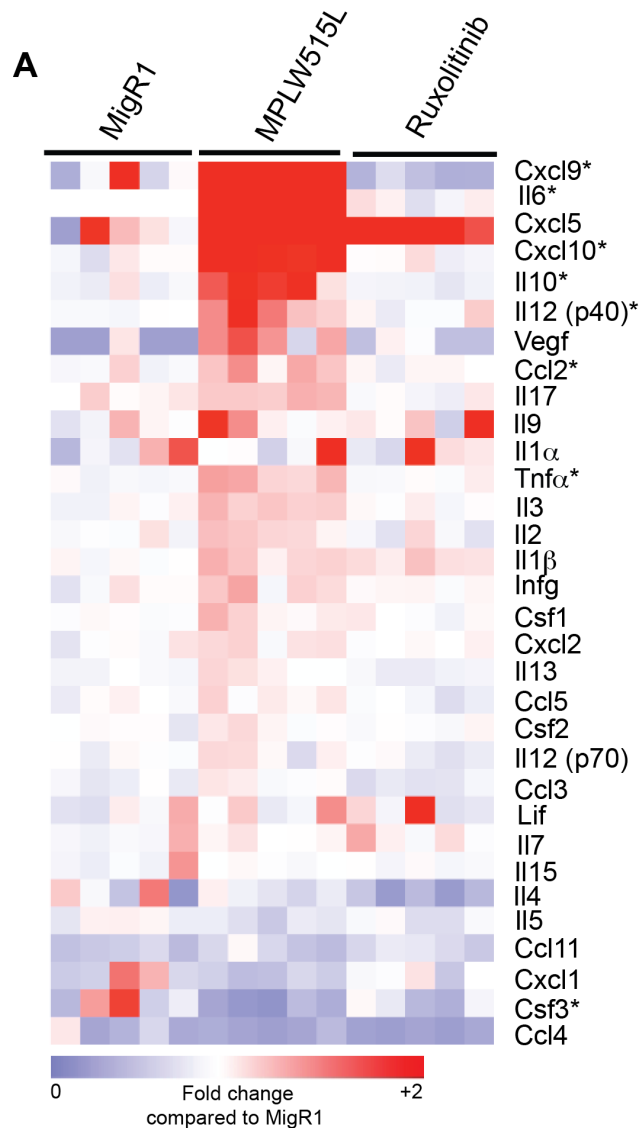
¹⁰Department of Pathology, Memorial Sloan-Kettering Cancer Center, New York, New York, USA

¹¹Yale Comprehensive Cancer Center, New Haven, CT

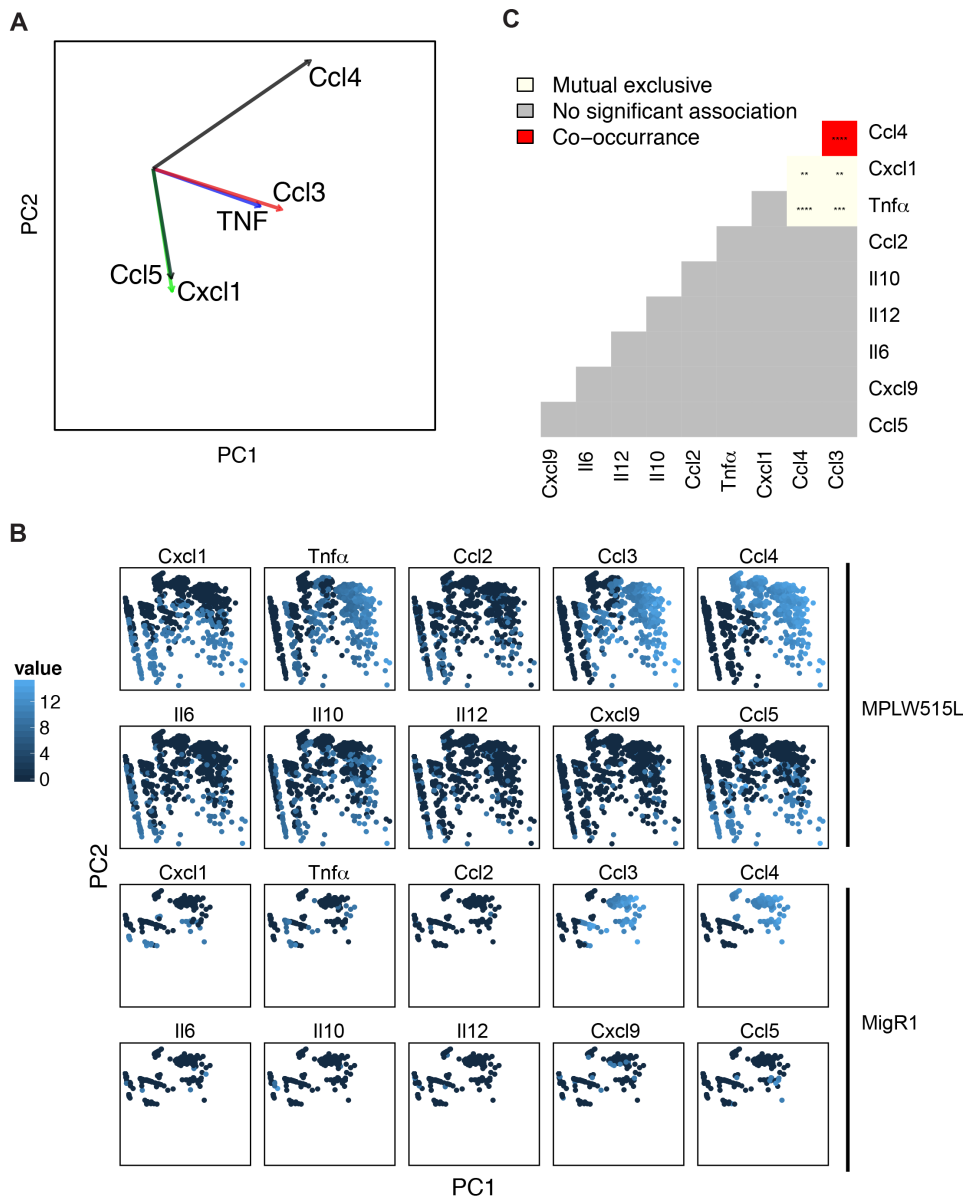
*These authors contributed equally to this work

Contents

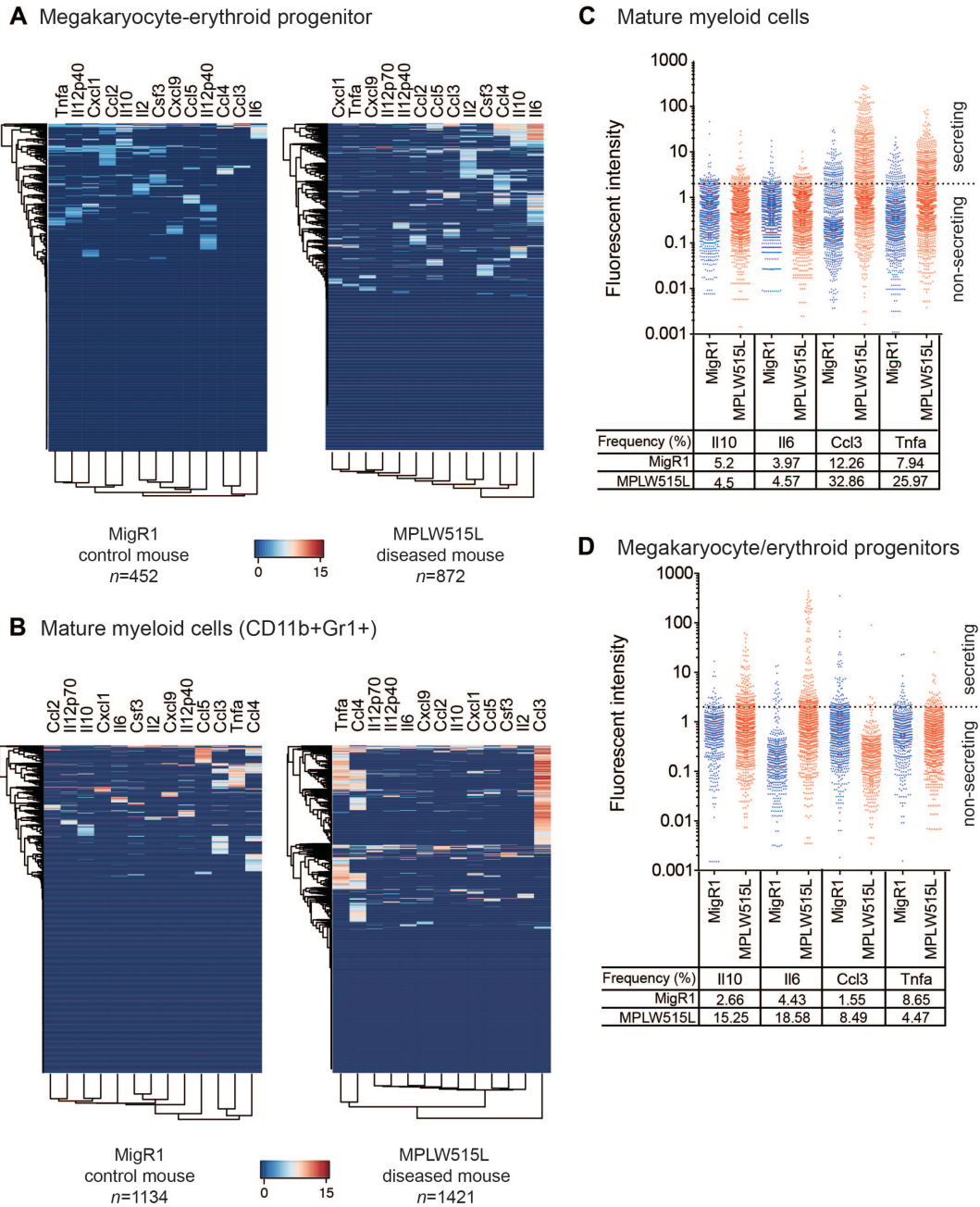
Supplementary Figures.....	p. 3-14
Supplementary Figure 1.	p. 3
Supplementary Figure 2.	p. 4
Supplementary Figure 3.	p. 5
Supplementary Figure 4.	p. 6
Supplementary Figure 5.	p. 7
Supplementary Figure 6.	p. 8
Supplementary Figure 7.	p. 9
Supplementary Figure 8.	p. 10
Supplementary Figure 9.	p. 11
Supplementary Figure 10.	p. 12
Supplementary Figure 11.	p. 13
Supplementary Figure 12.	p. 14
Supplementary Figure 13.	p. 15
Supplementary Figure 14.	p. 16
Supplementary Figure 15.	p. 17
Supplementary Tables.....	p. 18
Supplementary Table. 1	p. 18
Supplementary Table. 2	p. 19



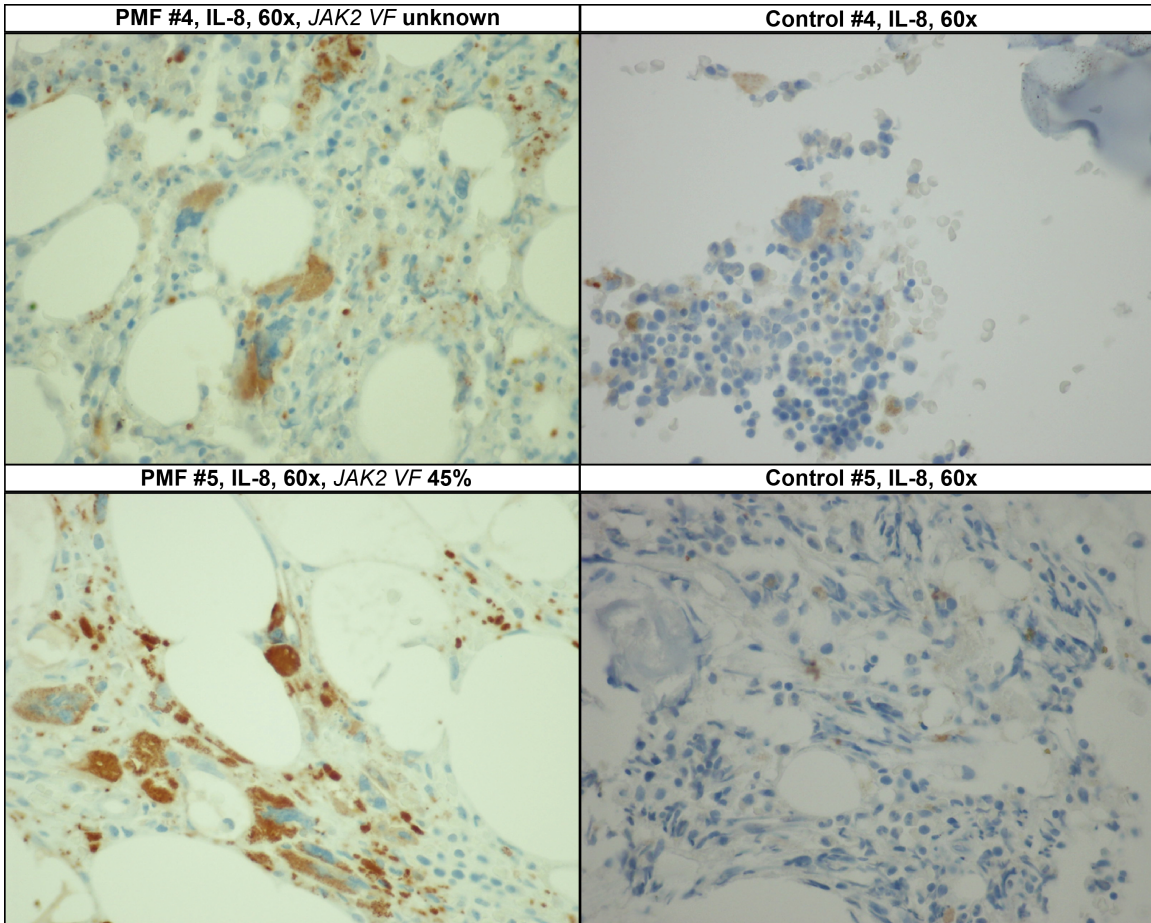
Supplementary Figure S1 | Pro-inflammatory cytokines are elevated in MF mice and reversed with JAK inhibitor treatment. Displayed are fold changes in serum cytokines levels in vehicle-treated MPLW515L (MPLW515L) mice after 14 days of treatment compared with levels in control (MIGR1) Balb/c mice, as well as serum cytokine levels in MPLW515L mice treated with 14 days of 90 mg/kg ruxolitinib. * Statistically significant cytokines selected for future studies. *n*=5 in each group.



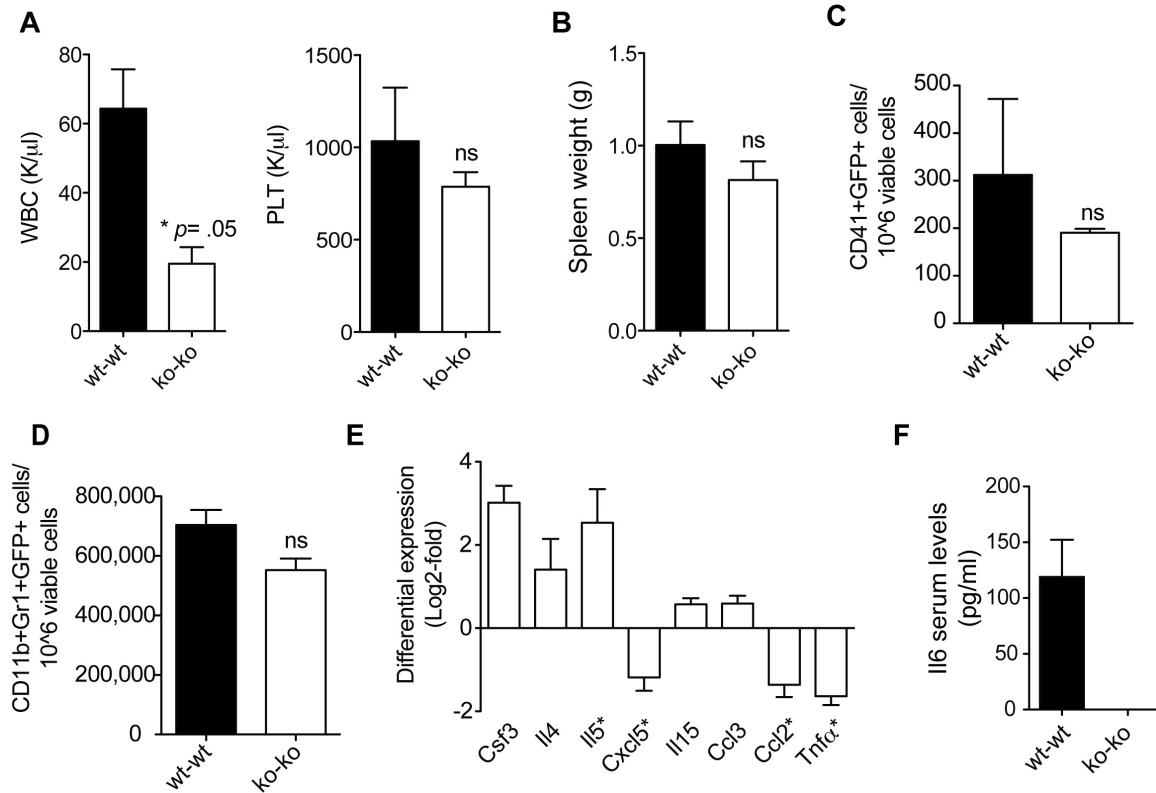
Supplementary Figure S2 | Principal component analysis of MF cells. **A**, Principal component analysis (PCA) of single cell cytokine secretion data from MPLW515L and control cells identified two principal components, PC1 and PC2, largely defined by production of cytokines Tnf α , Ccl3, and Ccl4 (PC1) and Cxcl1 and Ccl5 (PC2). **B**, PCA of MPLW515L (upper panel) and healthy control (lower panel) data for each cytokine are plotted separately. PCA map showing that a large proportion of normal BM cells did not secrete any protein while there are a number of small subsets with distinct secretion patterns, producing only 1-2 cytokine, most notably, CCL3 and CCL4. In contrast, BM cells from MF mice were divided into non-producers, producers of CCL3, CCL4 and TNF α , producers of CCL5 and CXCL1, and multifunctional cells that produce elevated levels of diverse inflammatory cytokines. Colors indicate the log-transformed measurements for each cytokine. **C**, Mutual exclusivity analysis for control cells. Colors indicate FDR. Pairs of cytokines displaying statistically significant co-secretion are colored in red, and mutual exclusive pairs in light yellow. Pairs with co-secretion patterns with no statistically significant differences from randomly expected patterns are shown in grey.



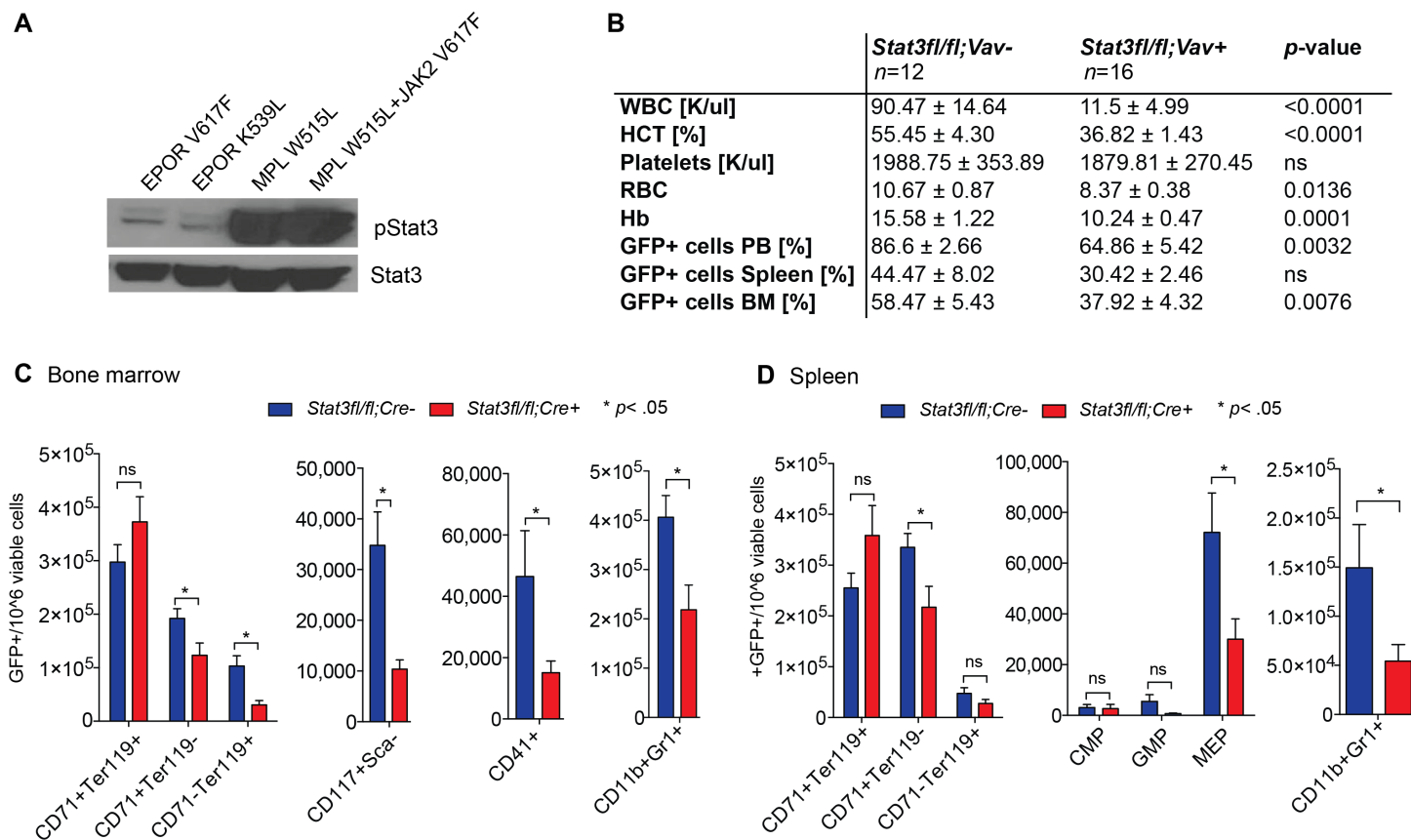
Supplementary Figure S3 | Single cell analysis of immunophenotypically-defined subpopulations from MF and control mice. **A, B,** Hierarchical cluster analysis of single cell data (log-transformed) of GFP-positive megakaryocyte/erythroid progenitor (MEP) (**A**) and mature CD11b+Gr1+ myeloid (**B**) BM cells depicting increase in the cytokine production levels and the degree of heterogeneity of both immunophenotypic-defined subpopulations. MigR1-transplanted mice are shown as control. *n*=number of single cells analyzed in this experiment. **C, D,** Vertical dot blot displaying normalized fluorescent intensity for four different cytokines (Il10, Il6, Ccl3 and Tnfa). Numbers in table below show cytokine secretion frequency [%] for each cytokine and group. Dotted lines indicate cytokine secretion threshold. Cells above this line are considered as cytokine secreting cell for a respective cytokine.



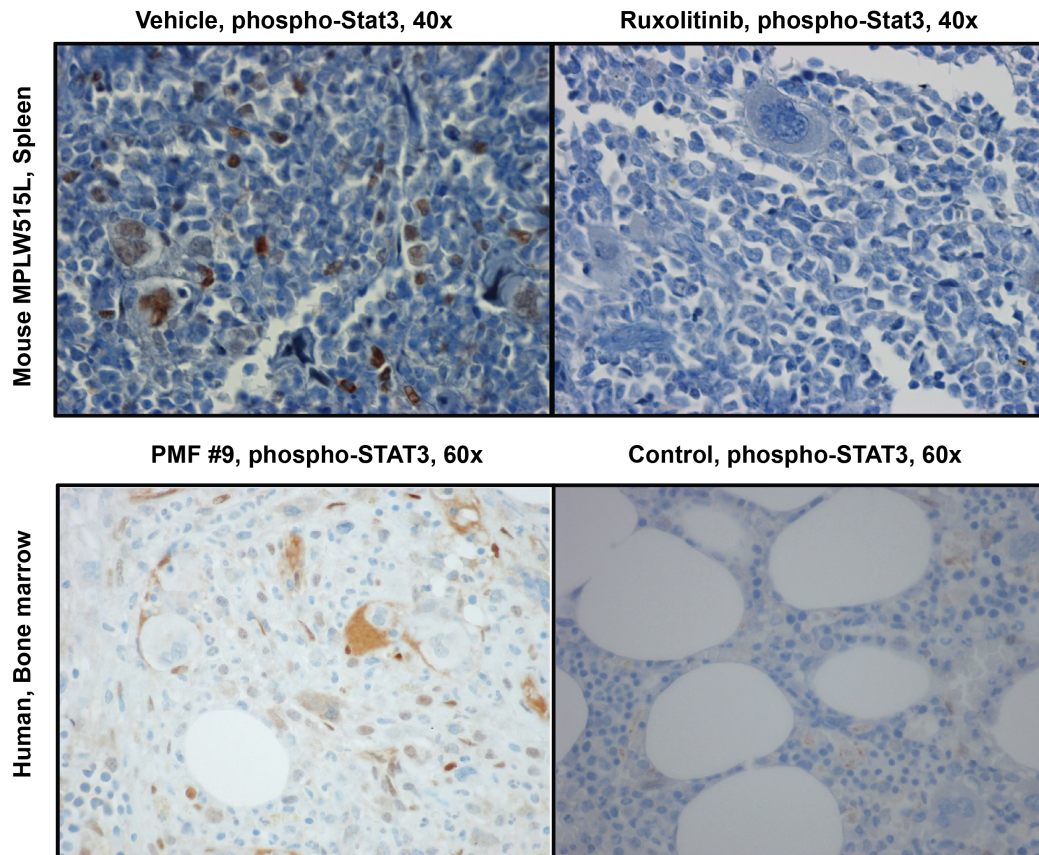
Supplementary Figure S4 | Elevated IL8 expression in MF patients. BM biopsies from primary MF patients were stained for IL8. Images (60x) of two representative cases are displayed. Bone marrow samples from three individuals without neoplasia or malignancy were used as normal controls. PMF: primary myelofibrosis, *JAK2 VF*: *JAK2 V617F* allele burden.



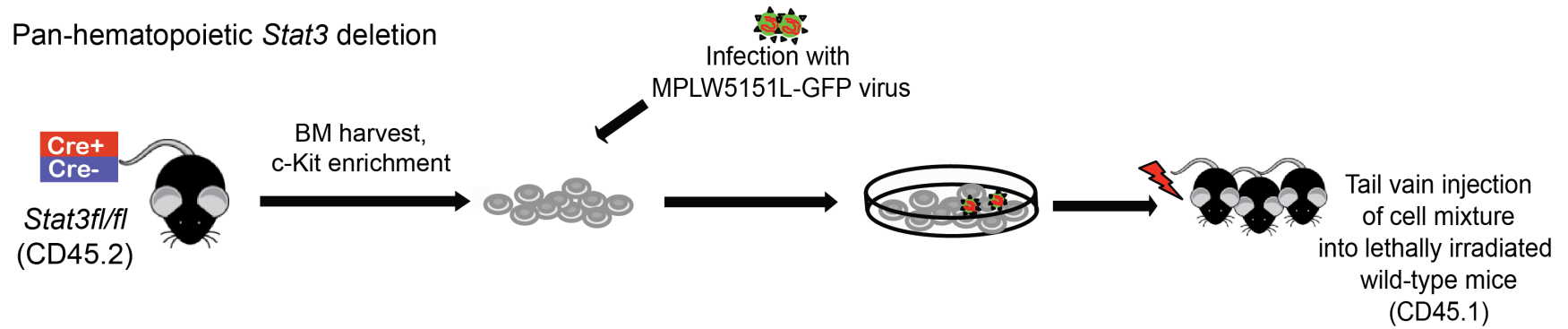
Supplementary Figure S5 | Complete removal of Il6 from the mouse system shows only minor effects on MPLW515L disease. **A**, MPLW515L-diseased Il6-deficient mice show reduced leukocytosis compared to control mice. (“wt-wt” indicates transfection of wild-type BM with MPLW515L-GFP virus and transplantation into wild-type recipients while “ko-ko” indicates transfection of *Il6*-deficient BM with MPLW515L-GFP virus into *Il6*-deficient recipients). **B** Absence of *Il6* does not affect splenomegaly in the MPLW515L mouse model. **C**, **D**, Flow cytometric analysis reveals no difference between mice with and without expression of Il6. CD41+, megakaryocytes (C), CD11b+Gr1+, myeloid population (D). **E**, Cytokine profiling using the Luminex platform shows compensatory changes in different cytokines (Il4, Il5) in MPLW515L- diseased mice lacking *Il6*. Log2-fold change is shown. * $p < .05$ e, Luminex data confirming complete lack of Il6 in the serum of knock-out to knock-out MPLW515L-transplanted mice. wt, wild-type, ko, knock-out. $n=6$ /group. Mean \pm s.e.m. are shown.



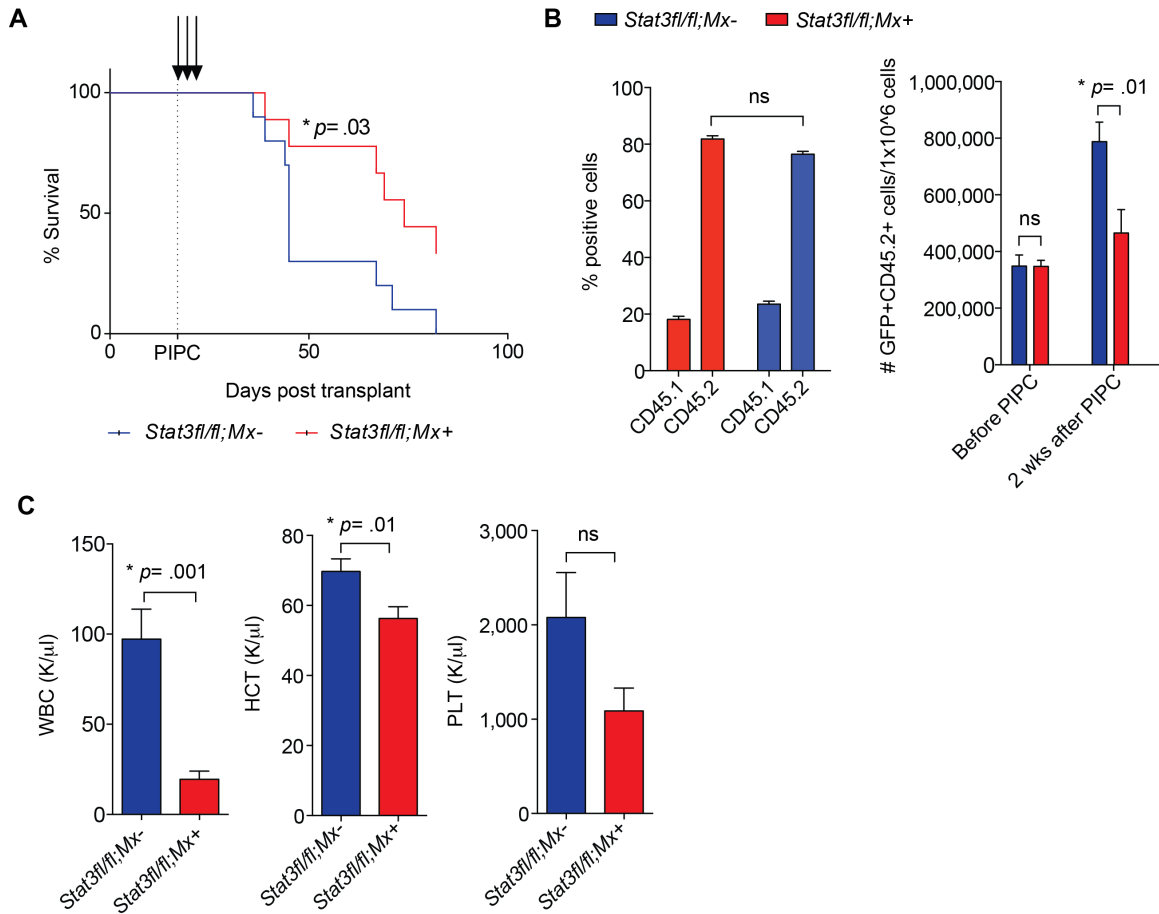
Supplementary Figure S6 | Peripheral blood and cytometric flow analysis of MPLW515L transplanted mice with and without *Stat3* deletion. **A**, Analysis of signal transduction in Ba/F3 cells expressing EPOR-JAK2V617F, EPOR-JAK2K539L, MPLW515L-JAK2V617F, and MPLW515L. **B**, Differential blood counts of diseased mice which were transplanted with *Stat3fl/fl;Cre-Vav+* or *Stat3fl/fl;Cre-Vav-* MPLW515L transduced bone marrow. *Cre-Vav+*: *n*=7, *Cre-Vav-*: *n*=10. **C**, **D**, Flow cytometric analysis of BM (**C**) and spleen cells (**D**) illustrating reduced numbers of GFP-positive (GFP+) megakaryocyte/erythroid progenitor cells (MEP), megakaryocytes (CD41+), myeloid cells (CD11b+Gr1+), erythroid (CD71/Ter119), and CD117-positive cells. GMP, *granulocyte/monocyte progenitors*, CMP, *common-myeloid progenitors*. *n*=12 for *Cre-Vav-* group, *n*=16 for *Cre-Vav+* group. Mean ± s.e.m. are shown.



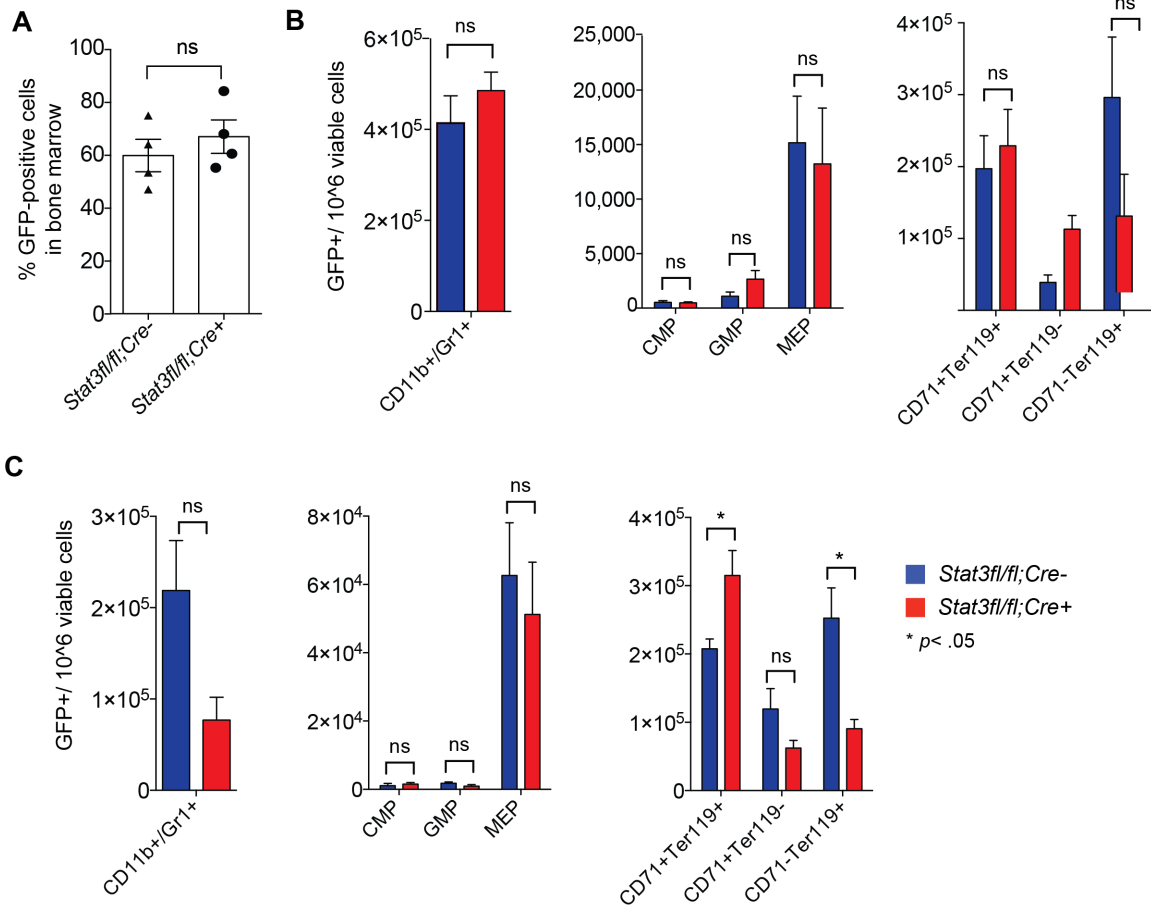
Supplementary Figure S7 | Constitutive activation of STAT3 in the BM of MPLW515L mice and primary MF patients. A, Immunohistochemical (IHC) analysis showed constitutive activation of Stat3 in the spleen of MPLW515L-diseased mice (left) which was inhibited by chronic JAK inhibitor treatment (right). Magnification 40x. **B,** IHC analysis of bone marrow biopsies from PMF patients showed increased nuclear expression of activated STAT3 in myeloid and endothelial cells and cytoplasmic localization to megakaryocytes compared to control bone marrow. Magnification, 60x.



Supplementary Figure S8 | Schematic illustration of bone marrow transplantation experiments using *Stat3*-deficient mice or littermate control mice as donors. Pan-hematopoietic deletion of *Stat3*. For these experiments, we harvested BM cells from *Stat3^{fl/fl}; Cre-Vav⁺* and *Stat3^{fl/fl}; Cre-Vav⁻* donors, enriched for HSPCs by using c-Kit enrichment. C-Kit-positive cells were then infected with retroviral MSCV-*hMPLW515L*-IRES-GFP or empty MSCV-IRES-GFP vectors. 1×10^6 cells were injected into the tail veins of syngeneic wild-type mice.

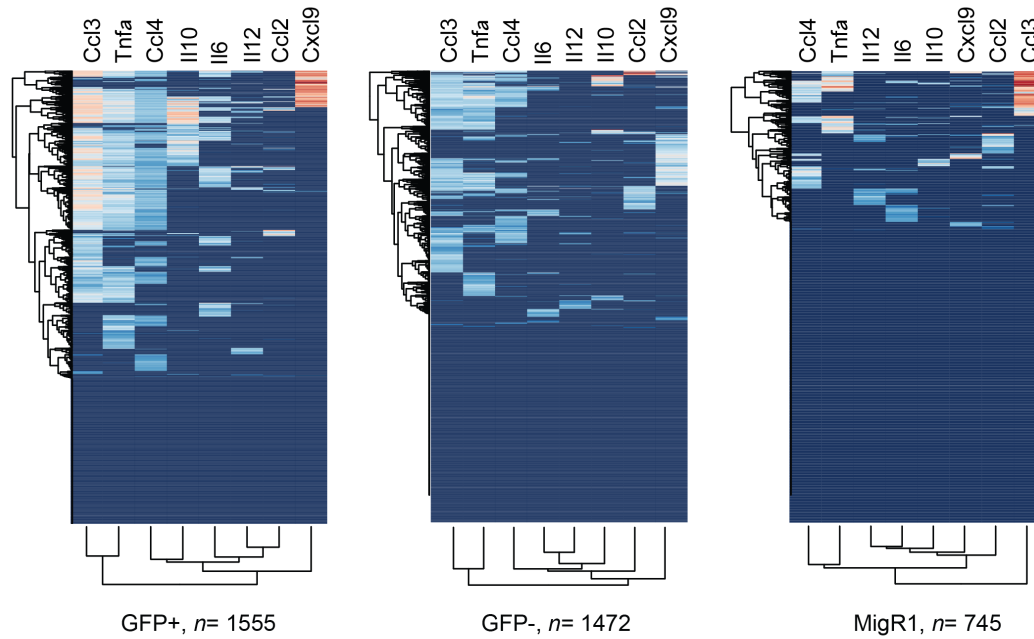


Supplementary Figure S9 | Excision of *Stat3* post engraftment prolongs survival and reduces leukocytosis. **A**, MPLW515L-transplanted recipient mice received three doses of *poly(I)–poly(C)* (PIP) post engraftment (d17, d19, d21) to induce expression of Cre recombinase from the *Mx-Cre* promoter. Mice receiving *Stat3fl/fl;Cre-Mx+* bone marrow cells survived significantly longer compared to *Stat3fl/fl;Cre-Mx-* cells. Survival curves a representative transplant are shown. $n=10$ mice for each group. **B**, Flow cytometric analysis illustrating equal numbers of CD45.2 donor cells engrafted in lethally irradiated CD45.1 recipient mice before excision of *Stat3* (left panel). GFP-levels within the CD45.2 cell compartment are lower in *Stat3fl/fl;Cre-Mx+* mice compared to *Stat3fl/fl;Cre-Mx-* mice at two weeks post PIP. **C**, Excision of *Stat3* post engraftment results in lower white blood cell (WBC) count and reduced hematocrit (HCT). PLT, platelets.

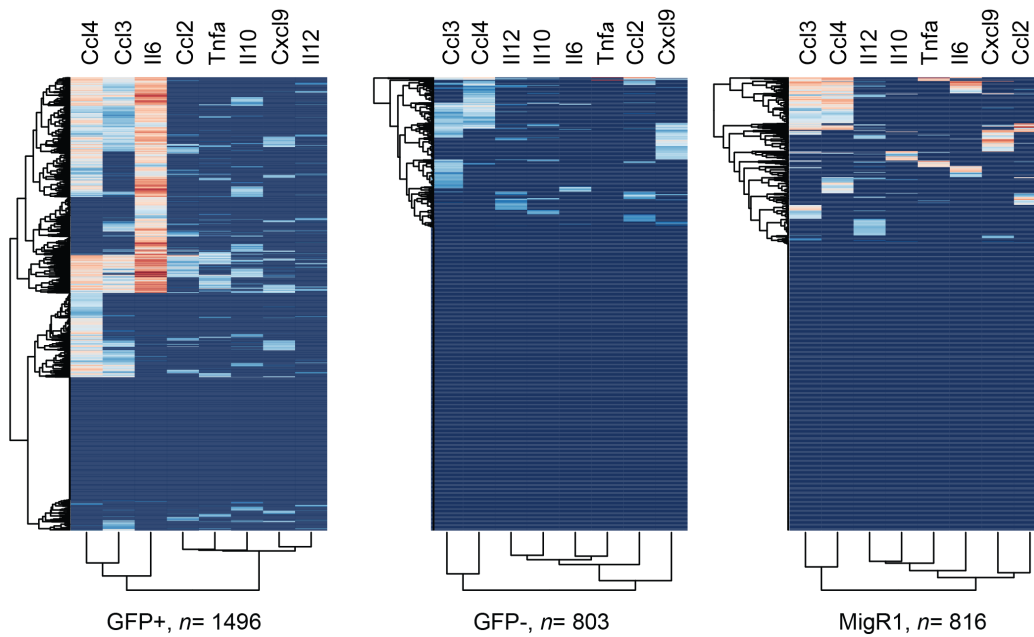


Supplementary Figure S10 | Mutant-restricted deletion of *Stat3* does not affect disease severity *in vivo*. **A**, Flow cytometric analysis (GFP-expression) of BM cells from diseased mice. $n=10$ /group. **B**, **C**, Flow cytometric analysis of BM (**B**) and spleen (**C**) cells illustrating no statistically significant (ns) difference in the numbers of GFP-positive (GFP+) megakaryocyte/erythroid progenitor cells (MEP), megakaryocytes (CD41+), myeloid cells (CD11b+Gr1+), erythroid (CD71/Ter119), and CD117-positive cells. GMP, *granulocyte/monocyte progenitors*, CMP, *common-myeloid progenitors*. $n=4$ /*Cre-Vav-* group, $n=4$ /*Cre-Vav+* group. Mean \pm s.e.m. are shown.

A Lineage - positive bone marrow cells

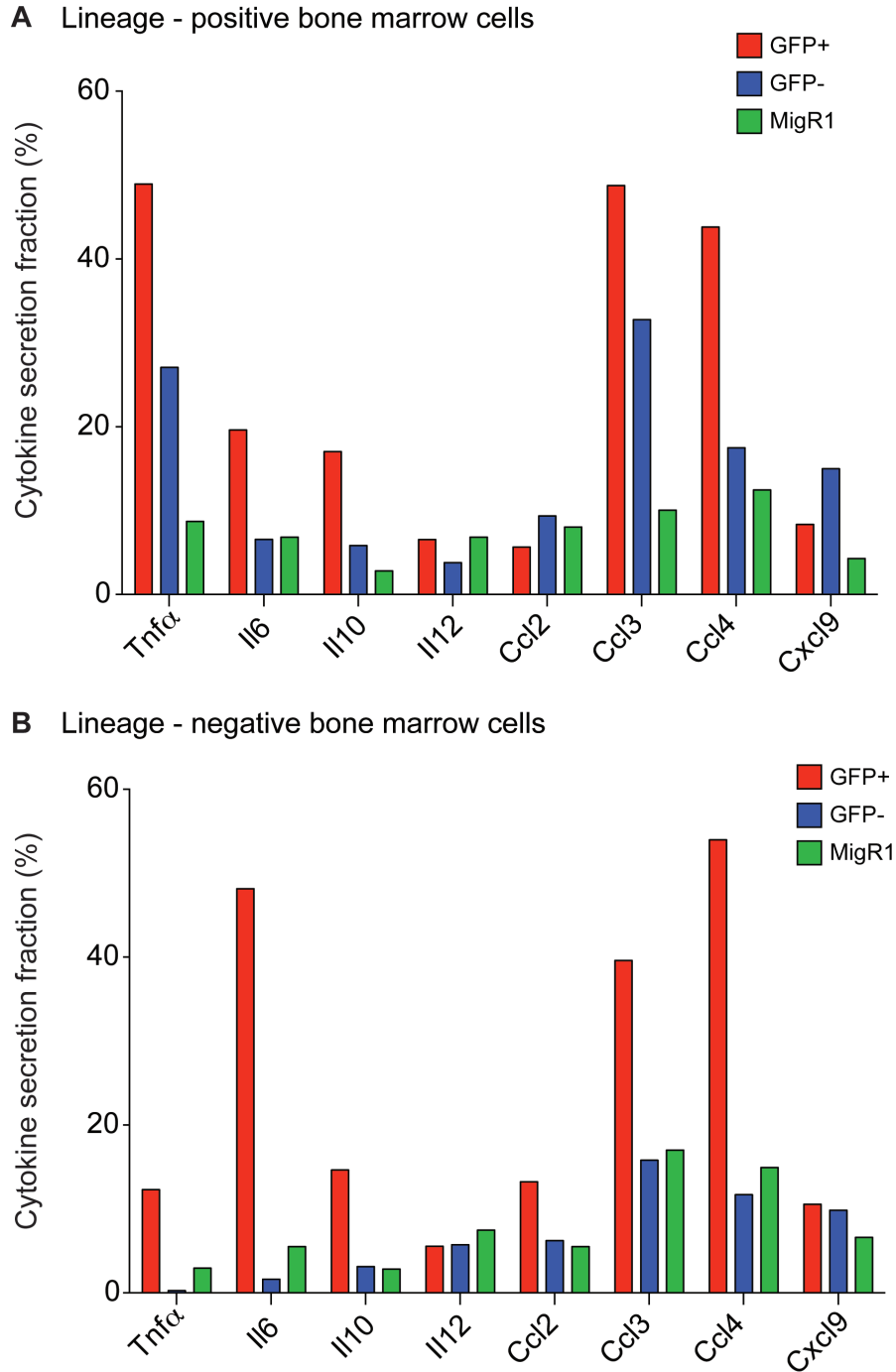


B Lineage - negative bone marrow cells

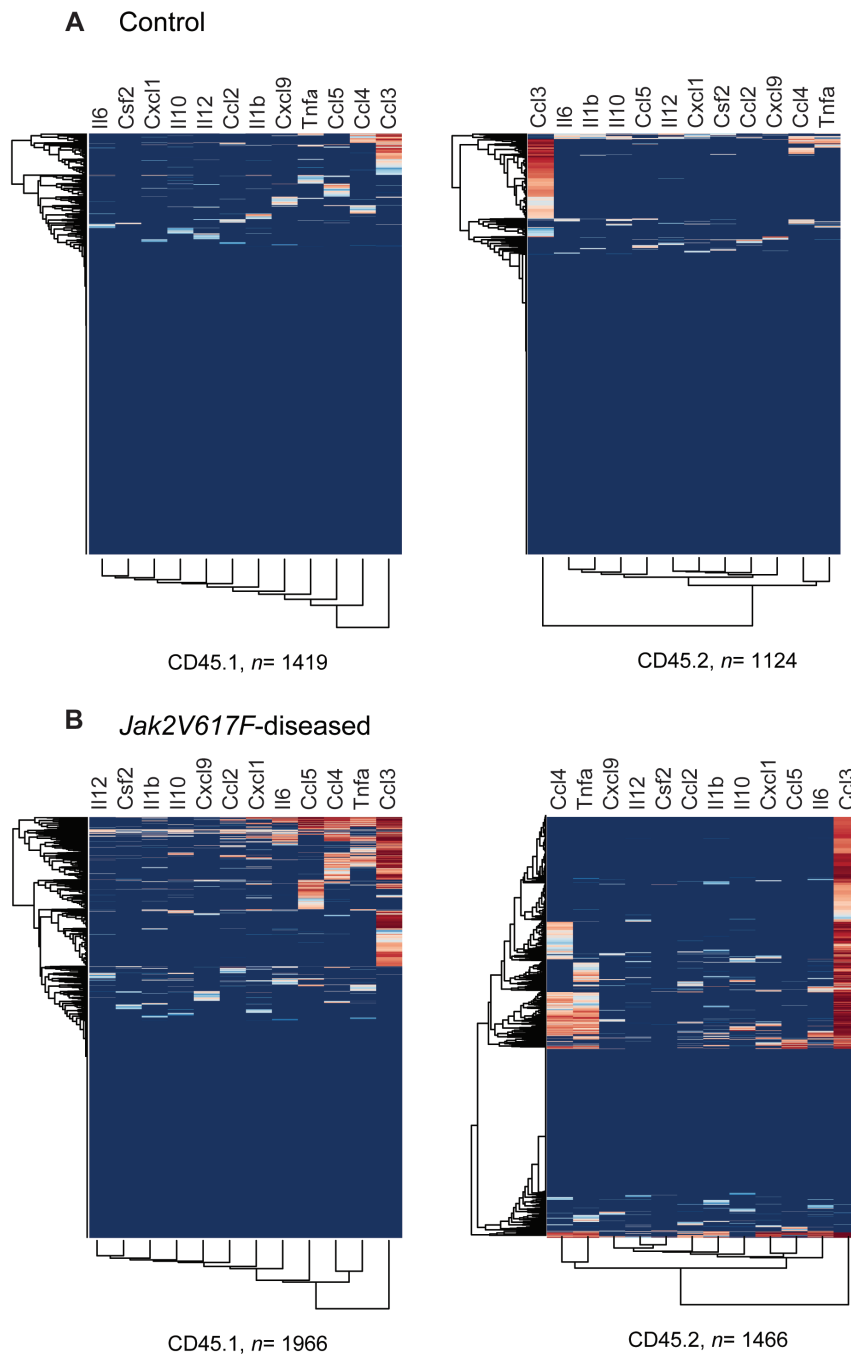


Supplementary Figure S11 | Single cell analysis of populations from MF and control mice.

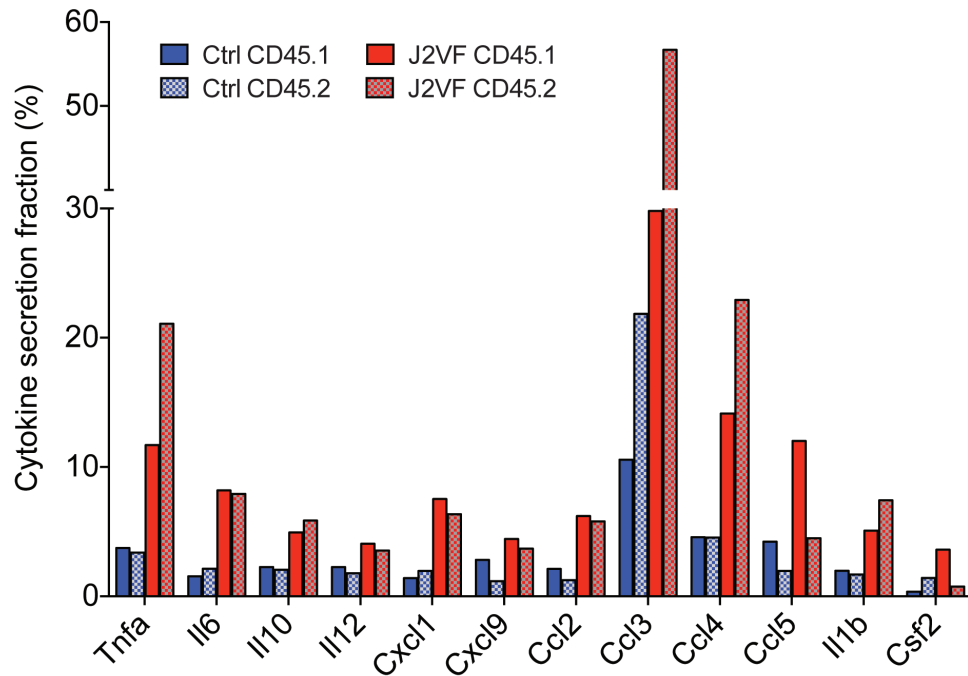
A, B, Hierarchical cluster analysis of single cell data (log-transformed) of lineage- positive (**A**) and lineage-negative (**B**) BM cells revealed a striking increase in the cytokine production levels and the degree of heterogeneity of both GFP-positive and GFP-negative MF cells compared to control cells. Unsorted lineage-positive and lineage-negative cells from MigR1-transplanted mice are shown as control. n =number of single cells analyzed in this experiment. GFP-positive: GFP+, GFP-negative: GFP-.



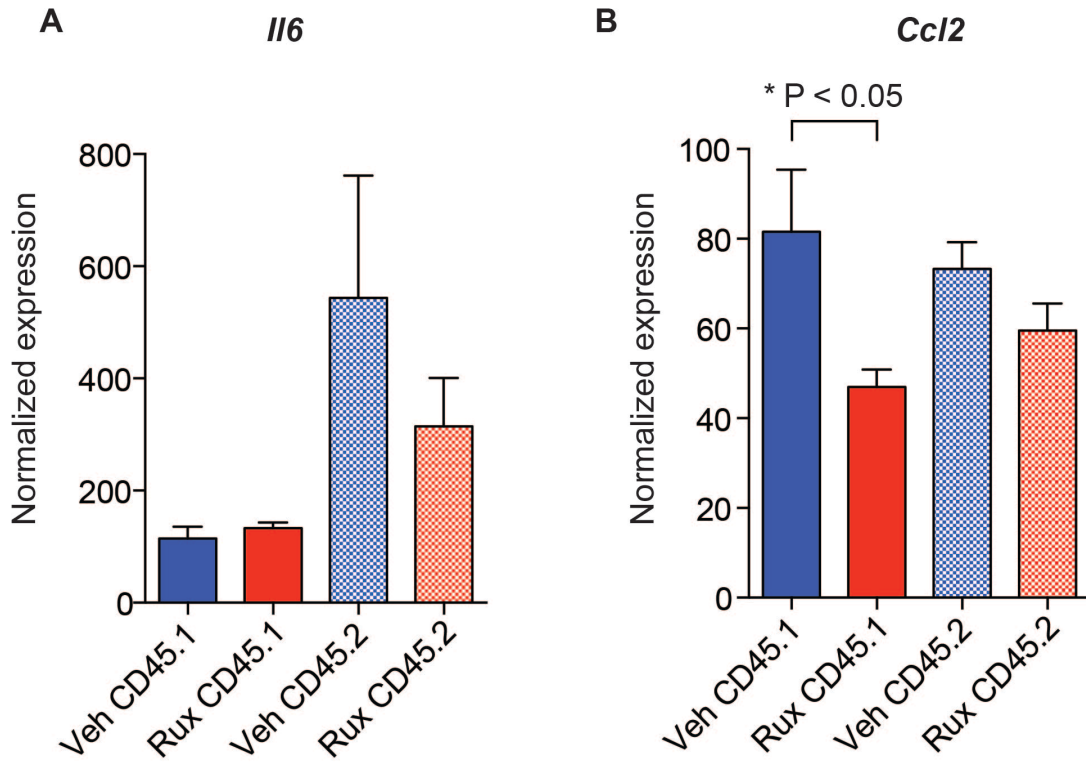
Supplementary Figure S12 | Mutant and non-mutant hematopoietic cells feature a higher percentage of cytokine secreting cells. A, B, The percentage of cells producing cytokines was higher in MPLW515L-derived lineage positive (**A**) and lineage-negative (**B**) GFP-positive (GFP+) and GFP-negative (GFP-) cells compared to healthy control cells (MigR1). All data are blotted. Lineage-positive GFP+: $n=1555$ cells, lineage-positive GFP-: $n=1472$ cells, lineage-positive MigR1: $n=745$ cells, lineage-negative GFP+: $n=1496$ cells, lineage-negative GFP-: $n=803$ cells, lineage-negative MigR1: $n=816$ cells.



Supplementary Figure S13 | Single cell analysis of populations from *Jak2V617F* MF and control mice. **A, B,** Hierarchical cluster analysis of single cell data (log-transformed) of CD45.1-positive (left panel) and CD45.2-positive (right panel) BM cells revealed a striking increase in the cytokine production levels and the degree of heterogeneity of both CD45.1-positive and CD45.2-positive MF cells (**B**) compared to control cells (**A**). Sorted CD45.1-positive and CD45.2-positive cells from Cre-transplanted mice are shown as control. n =number of single cells analyzed in this experiment.



Supplementary Figure S14 | Mutant and non-mutant hematopoietic cells feature a higher percentage of cytokine secreting cells. A, B, The percentage of cells producing cytokines was higher in *Jak2V617F*-derived (J2VF) CD45.1-positive, *Jak2* wild-type and CD45.2-positive, *Jak2V617F*-positive cells compared to respective populations in healthy control mice (Ctrl CD45.1 and Ctrl CD45.2). All data are blotted. Ctrl CD45.1 $n=1416$ cells, Ctrl CD45.2: $n=1124$ cells, J2VF CD45.1: $n=1966$ cells, J2VF CD45.2: $n=1466$ cells.



Supplementary Figure S15 | JAK1/2 inhibition reduces cytokine expression from CD45.1-positive wild-type cells and CD45.2-positive mutant cell population. A, B, NanoString expression data (mean ± s.e.m.) for CD45.1- and CD45.2 cells from vehicle/ruxolitinib-treated JAK2V617F-diseased mice. Veh: vehicle; Rux: ruxolitinib. *n*=4/group.

Supplementary Table 1. Primary myelofibrosis patient characteristics.

ID	<i>JAK2V617F</i> status	Application	IL8 expression level (IHC)	STAT3 phosphorylation status (IHC)
PMF#1	90%	Single cell	NA	NA
PMF#2	63%	Single cell	NA	NA
PMF#3	93%	Single cell	NA	NA
PMF#4	45%	IHC	2-3+	1-2+
PMF#5	Post transplant (no data)	IHC	2-3+	1-2+
PMF#6	100%	IHC	Focal 2-3+	1+
PMF#7	Negative	IHC	Focal 2+	1+
PMF#8	Negative	IHC	2+	0-1+
PMF#9	No data	IHC	3+	2+
PMF#10	Negative	IHC	1-2+	0-1+
PMF#11	38%	Single cell	NA	NA

PMF, primary myelofibrosis; IHC, immunohistochemistry; single cell; single cell cytokine secretion assay; NA, not applicable; IL8 expression levels and activation status of STAT3 were determined by IHC. *JAK2V617F* allele burden was determined using next-generation sequencing technologies (MiSeq or RainDance platform). IL8: 1-2+, negative to weak intensity; 2+, moderate intensity; 2-3+ moderate to marked intensity localization to myeloid cells, endothelial cells, platelets and megakaryocyte cytoplasm; normal bone marrow controls without neoplasia or malignancy showed rare megakaryocytes and platelets with weak IL8 expression. Phospho-STAT3, 0-1+, negative to weak intensity; 1+ weak intensity; 1-2+, weak to moderate intensity; 2+, moderate intensity localization to myeloid cells, endothelial cells or megakaryocytes; 2 normal bone marrow controls without neoplasia or malignancy showed rare myeloid or endothelial cells with weak phospho-STAT3 expression

Supplementary Table 2. Genetic alterations of patient PMF#11

<i>Gene</i>	<i>Exon</i>	<i>cDNA position</i>	<i>Amino acid change</i>	<i>Variant frequency</i>
<i>JAK2</i>	14	c.G1849T	p.V617F	38%
<i>CBL</i>	8	c.A1169T	p.D390V	17%
<i>IDH2</i>	1	c.T23C	p.V8A	45%
<i>ASXL1</i>	12	c.1904_1905delAG	p.R635fs	42%